附件一

行政院國家科學委員會補助專題研究計畫

□ 成 果 報 告
■期中進度報告

以電場變調紅外線吸收光譜學研究電場對水體及侷限空間水的效應

計畫類別：■ 個別型計畫　　□ 整合型計畫
計畫編號：NSC 98 - 2113 - M - 009 - 011 - MY2
執行期間：　98　年　8　月　1　日至　100　年　7　月　31　日

計畫主持人：重藤真介
共同主持人：
計畫參與人員：

成果報告類型(依經費核定清單規定繳交)：■精簡報告　□完整報告

本成果報告包括以下應繳交之附件：
□赴國外出差或研習心得報告一份
□赴大陸地區出差或研習心得報告一份
□出席國際學術會議心得報告及發表之論文各一份
□國際合作研究計畫國外研究報告書一份

處理方式：除產學合作研究計畫、提升產業技術及人才培育研究計畫、列管計畫及下列情形者外，得立即公開查詢
□涉及專利或其他智慧財產權，□一年□二年後可公開查詢

執行單位：國立交通大學應用化學系

中　華　民　國　99　年　5　月　25　日

Abstract (English)

The structure, dynamics, and properties of liquid bulk water are exceedingly complicated due to three-dimensional network of hydrogen bonds. Although a great deal of efforts has been devoted to understanding its anomalous characteristics, water still remains a mysterious substance to us. Water in confinement is more relevant to biology, because biological water is usually confined to organelles or cells with nano- to micrometer scale. However we know far less about water in confinement.

Here we study water in bulk and in confinement using infrared (IR) electroabsorption spectroscopy in order to shed more light on the mystery of water. This technique measures with high sensitivity changes in IR absorption intensity induced by an externally applied electric field modulation. It provides quantitative information on molecular properties such as the permanent dipole moment and the polarizability, which sharply reflect the structure and local environments of the molecule. Since H_2O is polar, it will respond to the electric field via dipolar interactions. If there is a thermal equilibrium between water molecules in distinct local hydrogen-bonding environments, equilibrium shift may also occur.

We have been studying IR electroabsorption of water with two approaches. In one approach, water dissolved in 1,4-dioxane has been investigated. We were able to detect the IR electroabsorption spectrum of the OH stretching of water, which is as small as 10^{-6} OD. The spectrum is indicative of an anomalously large change in the dipole moment and/or the polarizability upon vibrational excitation. In the other approach, AOT reverse micelles have been used to generate confined water. The IR electroabsorption spectrum of water in the AOT reverse micelle shows quite different features from what is observed for the 1,4-dioxane solution of water; it is likely to be caused predominantly by a change in equilibrium among at least three water species.

Keywords (English)

Infrared electroabsorption spectroscopy, bulk and confined water, liquid structure, reverse micelles

中文摘要

由於水分子間的氫鍵可以形成三維空間的網狀結構，造成群聚的水分子在結構、動力學以及液體性質的研究上極其複雜。雖然已有大量的研究致力於了解群聚水分子的不規則特性，但水分子對我們而言仍然是個未知的、神秘的物質。由於在生物體中的水分子，對於細胞器或細胞通常是受限制在奈米到微米尺度的，因此對於生物學而言，限制於此尺度範圍水分子的研究是更具有意義的。不過我們對於受尺度大小限制的水分子的了解卻相當少。

在此我們為了從水分子散射更多的光線來研究，我們用電場變調紅外線吸收光譜來研究有尺度大小限制的水分子和群聚水的分子。這套儀器系統測量調整外部施加的電場造成紅外線吸收強度的改變，且此儀器系統對於紅外線吸收強度的改變有高靈敏度；經由這套系統測量，可同時得到一些測量分子特性上定量的訊息，例如永久偶極矩和可極化度，而這些訊息也都清楚的反應了分子的結構和局部環境性質。由於水是極性的，所以經由偶極作用力可對外加電場做回應；如果水分子在不同氫鍵的局部環境中是有一個熱平衡的情況，那平衡的位移同樣會對外加電場做回應。

我們一直以來是從兩個途徑去研究水的電場變調紅外線吸收光譜，其中一個途徑是現在正在研究的將水溶解在 1,4-二氧陸圜中做測量，我們可以測量水分子 OH 鍵伸縮的電場變調紅外線吸收光譜，此樣品在我們的系統中吸收度的變化最小可測量到 10^{-6}，而

從光譜中指出在振動激發下，永久偶極矩和 / 或可極化度有一巨大的變化。另一個途徑是用 AOT 反微胞樣品來塑造受尺度大小限制的水分子，AOT 反微胞樣品和 1,4-二氧陸圜含水溶液的樣品兩者在電場變調紅外線吸收光譜展現出相當不同的特徵，這可能是直接由三種的水分子片段相互之間的平衡所造成的。

中文關鍵詞

電場變調紅外線吸收光譜（紅外線電場吸收光譜），群聚和受尺寸大小限制之水分子，液體結構，反微胞

報告內容

1. Introduction

The ultimate goal of this study is to answer the long-standing question in molecular science, of what water's structure and properties in bulk and in confinement are. Due to three-dimensional network of hydrogen bonds, liquid water exhibits anomalous thermodynamic behaviors[1], characteristic local environments, and ultrafast dynamics.[2] By way of example, the density of water reaches maximum at 4 ºC and decreases upon forming ice at 0 ºC. Ultrafast pump–probe spectroscopy has revealed[3-6] that the excitation of the OH stretching (ν_{OH}) vibration of water relaxes within 1 ps. In parallel with continuous research on bulk water, confined water has also attracted much attention recently.[7-9] In fact biological water should be viewed as being confined in nano- to micrometer scale. There have been many evidences that the dynamics occurring in confined water is substantially slower than that in bulk water.[7] Despite a great deal of efforts devoted in previous studies, a conclusive picture of bulk water and confined water has yet to be drawn.

In this project, infrared (IR) electroabsorption spectroscopy is used to study the molecular structure and intermolecular interactions of water at ambient temperature. This method is capable of observing changes in IR absorption intensity induced by an externally applied electric field as ΔA spectra and hence provides quantitative information on molecular properties including the permanent dipole moment μ_P and the polarizability α.[10-13] Since H_2O is a polar molecule, it is expected to respond to the applied field via dipole interactions. If there exist more than one water species in equilibrium reflecting distinct local environments, a change in the equilibrium would take place as well. However a technical problem arises from the intense ν_{OH} absorption.[14] Here we alleviate this problem by decreasing the concentration of water in two different ways. One approach is dilution with a solvent. In the present study, 1,4-dioxane is used as the solvent. The other approach is to confine water to the nanopool of the AOT reverse micelle.[9,15,16] We are able to control the size of the water pool by varying the molar ratio w_0 = [H_2O]/[AOT].[17] Not only does this technique effectively decrease water concentration, but it will allow us to compare the effect of confining water to the reverse micelle with that of dissolving water in a solvent.

2. Methods

A schematic of our IR electroabsorption spectrometer is shown in Fig. 1. The feature to note is the combined use of a dispersive IR monochromator and an AC-coupled signal amplifier, which can achieve sensitivity as high as $\Delta A \sim 10^{-7}$.[11,18] Our sample cell is also worth mentioning. It consists of a brass cell holder, two p-type boron-doped Si windows that

also act as electrodes, and a PET film spacer of ~6 μm thick.[11] This sample cell has made it possible to do IR electroabsorption spectroscopy of liquid samples at ambient temperature, in contrast to a series of measurements at 77 K by Boxer and co-workers.[13]

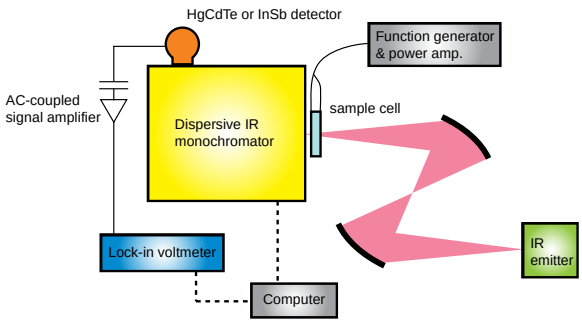

Fig. 1: Schematic of our IR electroabsorption spectrometer. In this work, an InSb detector was used.

3. Results and discussion

3.1. Water in 1,4-dioxane

Figure 2a displays a series of FT-IR spectra in the ν_{OH} region at 11 different concentrations of water dissolved in 1,4-dioxane. At 0.50 M, it is evident that the ν_{OH} spectrum consists of two major bands centered at around 3580 and 3510 cm^{-1}, and the 3580 cm^{-1} band is slightly more intense than the 3510 cm^{-1} band. As the concentration increases, the 3510 cm^{-1} band becomes stronger relative to the 3580 cm^{-1} band, concomitantly with emergence of the shoulder at ~3280 cm^{-1}. Thus there seems at least three ν_{OH} subbands involved in the concentration-dependent spectra. In order to verify this picture quantitatively, singular value decomposition[11,18] was employed. As shown in Fig. 2b, three major singular values are in fact obtained.

The ΔA spectrum of the 1.0 M solution is shown in Fig. 3a. The electric field strength of $F = 1.3 \times 10^7$ V m^{-1} was applied to the sample. Shown in Fig. 3b is the IR absorption spectrum measured with our dispersive monochromator. A least-squares fitting to sine

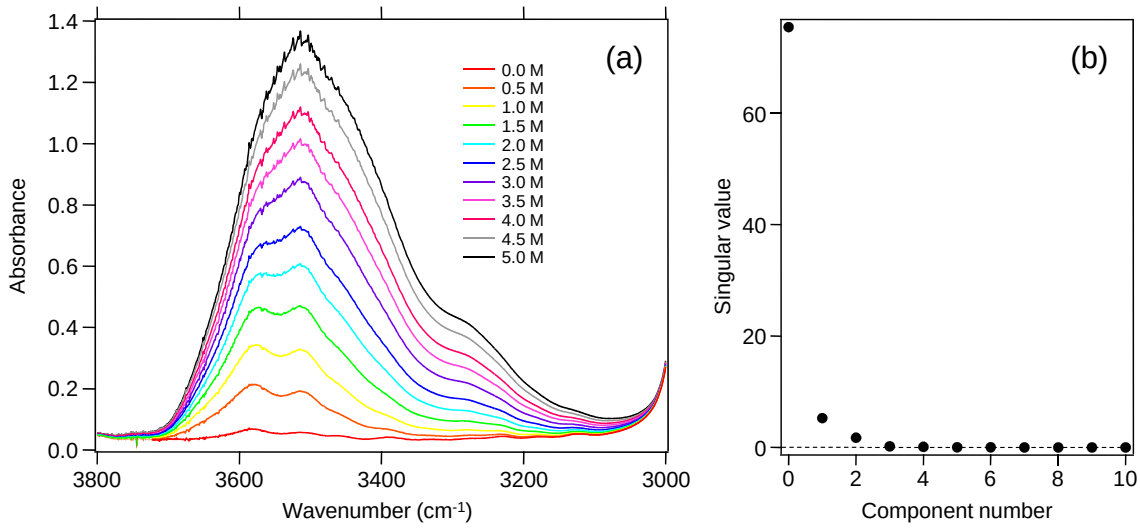

Fig. 2: (a) Concentration dependence of the FT-IR spectra in the ν_{OH} region, of water dissolved in 1,4-dioxane. The concentration of water varies from 0.0 to 5.0 M. (b) Singular values obtained from singular value decomposition of the FT-IR spectra in the ν_{OH} region.

function was performed to remove the baseline of the ΔA spectrum due to an interference fringe pattern. The baseline-subtracted ΔA spectrum is displayed in Fig. 3c. Although the signal-to-noise ratio (S/N) is not excellent, positive and negative features can be clearly seen at ~3540 and ~3600 cm^{-1}, respectively.

In general, the ΔA spectrum of a vibrational band, $\Delta A(\tilde{\nu})$, consists of the zeroth-, first-, and second-derivatives of the absorption band $A(\tilde{\nu})$:[19-21]

$$\Delta A(\tilde{\nu}) = F^2 \left[A_\chi A(\tilde{\nu}) + B_\chi \tilde{\nu} \frac{\mathrm{d}}{\mathrm{d}\tilde{\nu}} \left(\frac{A(\tilde{\nu})}{\tilde{\nu}} \right) + C_\chi \tilde{\nu} \frac{\mathrm{d}^2}{\mathrm{d}\tilde{\nu}^2} \left(\frac{A(\tilde{\nu})}{\tilde{\nu}} \right) \right] \quad (1)$$

where $\tilde{\nu}$ is the wavenumber, and A_χ, B_χ, and C_χ are, respectively, the coefficients of the zeroth-, first-, and second-derivative terms. χ represent the angle between the direction of the applied electric field and the electric field vector of the incident IR light. The ΔA spectrum shown in Fig. 3 was recorded at $\chi = 90°$. The zeroth-derivative component is attributed mainly to orientational anisotropy induced by the electric field,[11,18] while the first- and second-derivative components arise from electronic polarization[19-21] associated with changes in $\boldsymbol{\mu}_P$ and $\boldsymbol{\alpha}$ upon vibrational excitation.

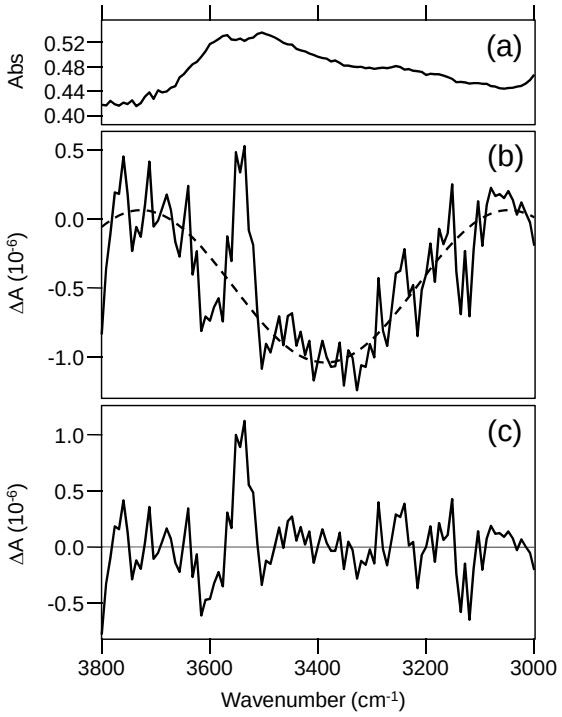

Fig. 3: (a) IR absorption spectrum in the ν_{OH} region, of water dissolved in 1,4-dioxane. The concentration of water was 1.0 M. (b) ΔA spectrum (solid curve) and the best fit of the baseline to sine function (dashed curve). (c) Baseline-subtracted ΔA spectrum.

The baseline-subtracted ν_{OH} ΔA spectrum was analyzed using Eq. 1. First, assuming that there are two components, the FT-IR spectrum of the 1.0 M solution was fit to a superposition of two Lorentzians. We used the FT-IR spectrum (Fig. 2a) rather than the IR spectrum measured with our IR electroabsorption

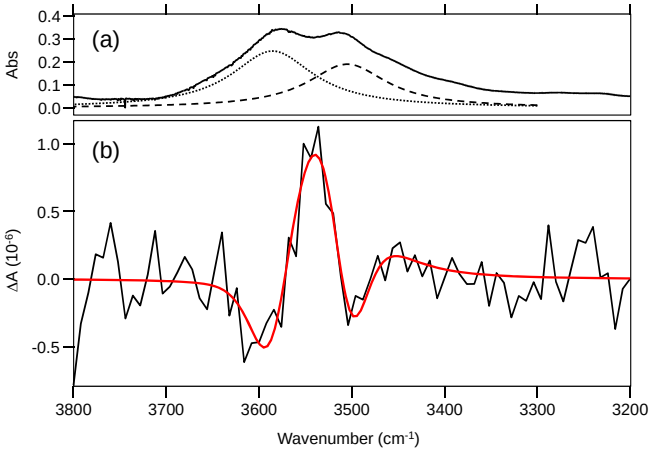

Fig. 4: (a) Spectral decomposition into two Lorentzians: components 1 (dotted) and 2 (dashed). (b) Fitting of the ΔA spectrum to the model function (Eq. 1).

spectrometer (Fig. 3a) simply because of a higher S/N. The decomposed Lorentzian bands are shown in Fig. 4. Hereafter the higher-wavenumber component will be denoted 1 and the lower-wavenumber 2. The best fit of the ΔA spectrum to Eq. 1 is also shown in Fig. 4. In the fitting, the peak position and the bandwidth for each component were fixed, leaving only the coefficients A_χ–C_χ adjustable parameters. The A_χ–C_χ thus determined are listed in Table 1. In contrast with our previous studies,[11,18] the contributions of the first- and second-derivative terms appear to be dominant, indicative of substantial changes in μ_P and/or α upon vibrational excitation.

TABLE 1: Coefficients A_χ, B_χ, and C_χ determined by the fitting

	Component 1	Component 2
A_χ	$-(2 \pm 1) \times 10^{-5}$	$(3 \pm 2) \times 10^{-5}$
B_χ	$(6 \pm 5) \times 10^{-4}$	$-(1.7 \pm 0.7) \times 10^{-3}$
C_χ	$(3.2 \pm 1.8) \times 10^{-2}$	$(5.7 \pm 1.5) \times 10^{-2}$

Those contributions depend in a different manner on the angle χ. The zeroth-derivative component originating from orientational polarization should vanish at $\chi = 54.7°$, and only the electronic polarization contribution remains. It is thus possible to separate those contributions by analyzing χ-dependence of the ΔA spectrum, which is now in progress.

3.2. Water in AOT reverse micelles

Figure 5 shows the ΔA spectrum of water in the $w_0 = 15$ AOT reverse micelle ([AOT] = 0.30 M), together with the absorption spectrum measured with a 50-μm spacer. The electric field strength was $F = 2.9 \times 10^6$ V m^{-1}. To estimate the mean diameter and size distribution of the reverse micelles, dynamic light scattering was also employed. The mean diameter d is obtained as $d = 6.4$ (±1.0) nm, which is in reasonable agreement with the estimation $d = 5.4$ nm, using the empirical formula[17] $d = 0.29w_0 + 1.1$ (nm) with $w_0 = 15$.

As shown in Fig. 5a, the absorption spectrum was fit to a sum of three Gaussian subbands. This contrasts with the case of water dissolved in 1,4-dioxane, where Lorentzians yield a better fit. Those subbands are thought of as corresponding to water molecules in different hydrogen-bonding states.[16,22,23] The subbands will be denoted H_1, H_2, and H_3 in order of increasing the frequency. With the peak position and the bandwidth of each subband fixed, the ΔA spectrum was then fit to a model function consisting of the zeroth-derivative shape of the absorption bands H_1–H_3 (see Fig. 5b). Both absorption and ΔA spectra are well reproduced by assuming the three subbands. A simple calculation shows that the orientational anisotropy signal for a water molecule[24] of $\mu_P = 1.85$ D is of the order of 10^{-7}, which is much smaller

than the observed signal, so the ΔA signal can be attributed solely to a change in the equilibrium that is assumed to exist among H_1–H_3. The absorbance change ratios for components H_1–H_3 are determined as $(\Delta A/A)_{H1} = 6.4 \times 10^{-5}$, $(\Delta A/A)_{H2} = 4.6 \times 10^{-5}$, and $(\Delta A/A)_{H3} = -3.3 \times 10^{-6}$, respectively. Obviously the sum of these ratios does not equal zero. This is because the molar extinction coefficients for subbands H_1–H_3 are different due to different hydrogen-bonding configurations. The signs of $\Delta A/A$ for H_1–H_3 suggest that applying an electric field may cause hydrogen bonds to break (or weaken), giving rise to apparent increase in the "bound water" (H_1 and H_2) and decrease in the "bulk water" (H_3).[16,25-27] The w_0 dependence of the ΔA spectrum will be examined in order to provide more solid evidence.

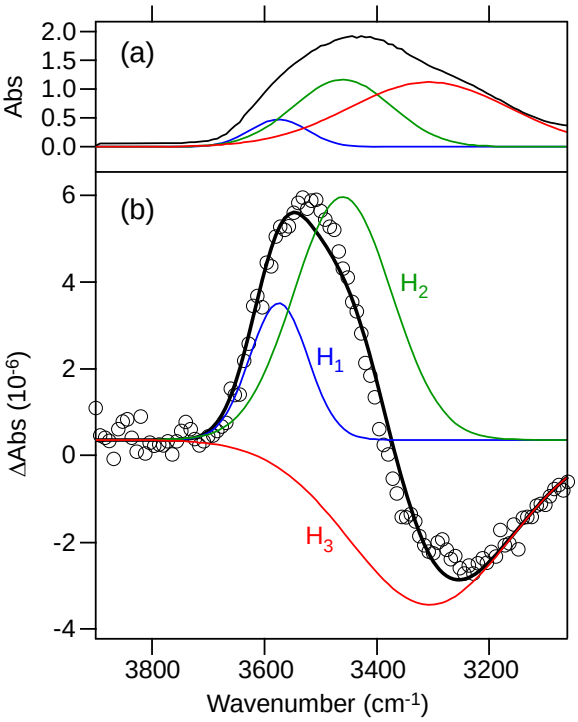

Fig. 5: (a) ν_{OH} spectrum of water in the $w_0 = 15$ AOT reverse micelle. The spectrum was fit to a superposition of three Gaussians (H_1, H_2, and H_3). (b) Observed ΔA spectrum (circles) and the best fit to the model function (black solid curve, see text for details).

參考文獻

1. D. Eisenberg and W. Kauzmann, *The Structure and Properties of Water*, Oxford Univeristy Press, London, 1969.
2. E. T. J. Nibbering and T. Elsaesser, *Chem. Rev.* **104**, 1887 (2004).
3. S. Woutersen, U. Emmerichs, and H. J. Bakker, *Science*, **278**, 658 (1997).
4. C. J. Fecko, J. D. Eaves, J. J. Loparo, A. Tokmakoff, and P. L. Geissler, *Science*, **301**, 1698 (2003).
5. M. L. Cowan, B. D. Bruner, N. Huse, J. R. Dwyer, B. Chugh, E. T. J. Nibbering, T. Elsaesser, and R. J. D. Miller, *Nature*, **434**, 199 (2005).
6. Z. Wang, Y. Pang, and D. D. Dlott, *J. Phys. Chem. A* **111**, 3196 (2007).
7. J. J. Gilijamse, A. J. Lock, and H. J. Bakker, *Proc. Natl. Acad. Sci. USA* **102**, 3202 (2005).
8. H.-S. Tan, I. R. Piletic, R. E. Riter, N. E. Levinger, and M. D. Fayer, *Phys. Rev. Lett.* **94**, 057405 (2005).
9. J. C. Dèak, Y. Pang, T. D. Sechler, Z. Wang, and D. D. Dlott, *Science*, **306**, 473 (2004).
10. A. Chattopadhyay and S. G. Boxer, *J. Am. Chem. Soc.* **117**, 1449 (1995).
11. H. Hiramatsu and H. Hamaguchi, *Appl. Spectrosc.* **58**, 355 (2004).
12. T. Nakabayashi and N. Ohta, *Chem. Lett.* **34**, 1194 (2005).
13. S. G. Boxer, *J. Phys. Chem. B* **113**, 2972 (2009).
14. J. E. Bertie and Z. Lan, *Appl. Spectrosc.* **50**, 1047 (1996).
15. N. Levinger, *Science*, **298**, 1722 (2002).
16. G. Onori and A. Santucci, *J. Phys. Chem.* **97**, 5430 (1993).
17. T. Kinugasa, A. Kondo, S. Nishimura, Y. Miyauchi, Y. Nishii, K. Watanabe, and H. Takeuchi, *Colloids Surf. A* **204**, 193 (2002).
18. S. Shigeto, H. Hiramatsu, and H. Hamaguchi, *J. Phys. Chem. A* **110**, 3738 (2006).
19. W. Liptay, *Angew. Chem. Int. Ed.* **8**, 177 (1969).
20. M. Ponder and R. Mathies, *J. Phys. Chem.* **87**, 5090 (1983).
21. G. U. Bublitz and S. G. Boxer, *Annu. Rev. Phys. Chem.* **48**, 213 (1997).
22. A. Rahman and F. H. Stillinger, *J. Chem. Phys.* **55**, 3336 (1971).
23. R. Laenen, R. Rauscher, and A. Laubereau, *J. Phys. Chem. B* **102**, 9304 (1998).
24. S. A. Clough, Y. Beers, G. P. Klein, and L. S. Rothman, *J. Chem. Phys.* **59**, 2254 (1973).
25. N. V. Nucci and J. M. Vanderkooi, *J. Phys. Chem. B* **109**, 18301 (2005).
26. S. Balakrishnan, N. Javid, H. Weingärtner, and R. Winter, *ChemPhysChem*, **9**, 2794 (2008).
27. T. K. Jain, M. Varshney, and A. Maitra, *J. Phys. Chem.* **93**, 7409 (1989).

計畫成果自評

To achieve the goal of this project, we have been using two approaches: IR electroabsorption studies of water dissolved in 1,4-dioxane and of water in AOT reverse micelles. In both approaches, we have successfully detected electroabsorption signals of water with fairly good signal-to-noise ratios. To the best of our knowledge, those data are the first observation of water's responses to an externally applied electric field.

In the second year of the project, we will perform more experiments such as the angle χ dependence for water in 1,4-dioxane and the w_0 dependence for water in the reverse micelle. We will then analyze our data to obtain quantitative information on the liquid structure of bulk water and confined water. Better understanding of water will impact a multitude of interdisciplinary areas. We hope to publish our results in journal(s) with a broad readership.